PROCEEDINGS REPRINT

SPIE–The International Society for Optical Engineering

Reprinted from

Fiber Optic and Laser Sensors XII

25–27 July 1994
San Diego, California

Volume 2292

Fiber optic interferometric sensors for aeroacoustic measurements: Anechoic chamber tests

Y. C. Cho and M. G. Bualat

NASA Ames Research Center, Mail Stop 269-3
Moffett Field, California 94035-1000

ABSTRACT

We report here progress on a NASA program to develop fiber optic interferometric sensors for aeroacoustic measurements. As reported earlier, NASA's first fiber-optic microphone was developed and fabricated. Preliminary anechoic chamber tests demonstrated successfully its feasibility as an aeroacoustic sensor. Improved performance of a newly designed sensor head is presented here in terms of frequency response function and noise floor.

1. INTRODUCTION

Acoustic measurements in wind tunnels are subject to certain interference effects which are not found in anechoic chambers. Such effects include wind noise, flow-sensor interaction noise, flow induced sensor vibration, deflection of acoustic waves by sensor induced boundary layers, reflections from facility and sensor support components, and noise due to temperature fluctuation. Currently existing acoustic sensor techniques are not adequate to cope with these problems. NASA Ames Research Center embarked on a program to develop new advanced acoustic sensors to eliminate or minimize these interference restrictions.[1-3] One element involves development of adaptive arrays using fiber optic (FO) sensors as transducers. The technology of FO interferometric sensors that has matured in underwater acoustics is adapted to aeroacoustics. FO acoustic sensors offer a number of advantages: high sensitivity, wide dynamic range, high temperature tolerance, compact sensor package, geometric versatility, superb telemetry capability, immunity to electromagnetic interferences, etc. The compact size of sensors can be utilized to reduce the flow-sensor interactions. Owing to its geometric versatility, the optical fiber can be configured with great flexibility as extended sensor elements or sensor arrays. Such configurations would generate a great variety of array sensitivity patterns. Furthermore, the optical fibers can be implanted on the surface of a solid body. With the sensor elements implanted on an aerodynamically smooth body, the flow-interaction can be made negligible, the aerodynamically induced vibration will be minimized, and effects of the boundary layer will be more tractable.

As previously reported,[2,3] a FO interferometric acoustic sensor was developed and fabricated in a breadboard form. Extensive anechoic chamber tests demonstrated its potential for aeroacoustic measurements in wind tunnels. The results showed that the signal to noise ratio was sufficiently large, but the frequency response function was somewhat unstable with fluctuation of 3 dB. The performance improvement with a newly designed sensor head is presented here in terms of noise floor and frequency response function.

2. APPROACH AND NEW SENSOR HEAD

Mach Zehnder interferometry was employed, as schematically illustrated in Fig. 1. The sensor is composed of a laser, a FO sensor head, an optical receiver, and a demodulator. The laser is frequency modulated with a modulating frequency of 10.4 kHz and a frequency amplitude of 1 MHz. The sensor head is made of single mode bare fiber wrapped around a **styrofoam** mandrel as schematically displayed in Fig. 2. During this investigation, it was learned that the acoustic sensitivity was attributed to fiber changes in length caused dominantly by the bulk expansion and contraction of the styrofoam mandrel. The mandrel expansion and contraction is induced by acoustic pressure, and the acoustic sensitivity is maximized as long as the linear dimension of the mandrel remains smaller than the wave length. The sensitivity due to fiber coating with

0-8194-1616-9/94/$6.00

acoustically sensitive material was at least 10 *dB* lower. As a consequence, the coated fiber which was used previously was replaced by bare fiber. This replacement allowed the same size of sensor head to be wrapped with longer fiber, giving rise to higher sensitivity. As illustrated in Fig. 2, the mandrel is 2.25 inches in length, and 1.75 inches in diameter. The sensing segment, which is the mandrel portion wrapped with fiber, is 1.25 inches long. This length holds 20 *m* of 250 μm diameter bare single mode fiber. The same length of the sensing segment would hold only 8 *m* of 630 μm diameter coated fiber as used in ref. 3.

3. TEST SETUP

Tests of the *FO* microphone were conducted in a small anechoic chamber which was built specifically for this program in the Photonics Laboratory, NASA Ames Research Center.

The anechoic chamber, whose plan view is schematically shown in Fig. 3, has the inner dimension 8 feet by 8 feet by 8 feet. The chamber was first lined with aluminum sheets to shield the inside from electromagnetic interference. Anechoic wedges which are 6 inches thick were then glued on the aluminum sheets. The wedges may not be thick enough to absorb sound of wave length longer than approximately one foot, equivalently of frequencies less than 1.1 kHz. However, the chamber needs not be expansively anechoic for the present tests that involve evaluations of noise floor and frequency response. The noise floor measurement requires the chamber to be well isolated acoustically rather than to be expansively anechoic. In this regard, this new chamber has advantages over the previously used National Full-scale Aerodynamic Complex Anechoic Chamber, which was often difficult to isolate from environmental noise generated from huge wind tunnels and auxiliary machinery. The frequency response function of the *FO* microphone was evaluated from the correlation of its measured acoustic field and a reference microphone measurement. Consequently, as long as the two microphones experience the same field, the reflection from the walls would not adversely affect tests. This condition can be satisfied pragmatically by placing the two microphones within a distance smaller than the wave length.

The reference microphone was a Brüel & Kjaer (*B&K*) condenser microphone of half an inch diameter. It was cantilevered from a strut of one inch diameter and 3 feet height as illustrated in Fig. 4. The *FO* microphone was placed directly under the *B&K* microphone. The vertical separation of the two microphones was about 2 inches from center to center. A Boston Acoustics loudspeaker was used as the source. It was an 8 *inches* diameter woofer with a frequency response covering 48 *Hz* to 20 *kHz* with 3 *dB* fluctuations. The speaker was placed on the top of a 3 feet high sound absorbing wedge block and 5 feet from the microphones.

The loudspeaker was driven by a Hewlett-Packard (*HP*) 3562A spectrum analyzer at frequencies between 20 *Hz* and 2.2 *kHz*. The frequency range was set in accordance with the operating frequency limit of the demodulator that was used for signal processing for the *FO* microphone. The demodulator was designed and fabricated for the Naval Research Laboratory in 1987,[4] and its frequency response function is shown in Fig. 5. The acoustic fields were simultaneously measured by the two microphones and processed by the *HP* spectrum analyzer for evaluation of the noise floor and the frequency response function.

The *B&K* microphone was calibrated using a standard piston-phone yielding an acoustic pressure level of 124 *dB* in reference to 20 μPa. To determine the absolute scale of the *FO* microphone measurement, a single-tone acoustic signal of 700 *Hz* was turned on during the noise floor measurement. The ordinate scale was so adjusted that the 700 *Hz* signal measured by the *FO* microphone would read the same magnitude as the *B&K* microphone measurement.

4. TEST RESULTS

The test results are presented in terms of the noise floor and the frequency response function. The noise floor is plotted as a function of frequency in Fig. 6, where the solid curve is used for the *FO* microphone and the

dotted for the *B&K* microphone. A single-tone signal of 700 *Hz* is present with the same magnitude for both of the microphones as marked with overlapped circles. The noise floor of the *FO* microphone is somewhat higher than that of the *B&K* microphone, but the difference decreases with increasing frequency. The difference is about 8 *dB* at 700 *Hz*, and appears to be negligible near 2 *kHz*. The noise floor of the *FO* microphone is lower than 20 *dB* re 20 μPa for frequencies above 200 *Hz*. Such a noise floor is far below the requirement for aeroacoustic measurements. One may notice that the noise floor of the *B&K* microphone does not exhibit the spurious single-tone signals at 60 *Hz* and its odd harmonics, which were present in the previously reported tests.[3] The reason is that the present tests were performed in the electromagnetically shielded anechoic chamber.

On the assumption of uniform frequency response of the *B&K* microphone, the frequency response function of the *FO* microphone was evaluated in terms of the transfer function, given by

$$H_{fb}(\nu) = \frac{G_{fb}(\nu)}{G_{bb}(\nu)}, \tag{1}$$

Here ν is the frequency, G_{bb} the acoustic power spectrum measured by the *B&K* microphone, and G_{fb} the cross spectrum of the two microphone measurements.

The frequency response function is plotted in its magnitude and phase in Figs. 7 and 8. The magnitude is the parameter that is useful for evaluation of microphone performance. It should be stable and remain unchanged from one measurement to another. The phase is used not only for evaluation of microphone reliability but also for evaluation of the test itself. Unlike for the noise floor, a linear frequency scale is used here to show the linear frequency dependence of the phase, which is as it should be. Two different acoustic sources were used for the frequency response function measurements - a random noise source and a swept sine mode. The random noise is wide band noise, and therefore the frequency response can be measured simultaneously for the whole frequency range. On the other hand, in a swept sine mode, a sine wave is stepped across the frequency span. Since the stepping speed is finite, the frequency response function is measured for different frequencies at different times.

The phase is discussed first. As plotted in Part b of Figs. 7 and 8, its frequency dependence is almost identical for both types of source. Except for frequencies near 300 *Hz* and 480 *Hz*, the phase decreases almost linearly with increasing frequency at a rate of 0.1875 *degrees/Hz*. This rate is greater than that for the demodulator, for which the phase decreases at a rate of 0.16 degrees/*Hz* as can be computed from Fig. 5b. This rate discrepancy of 0.0275 degrees/*Hz* was caused by the phase difference between the field measurements by the two microphones. As indicated in Fig. 4, the front ends of the two microphones are placed at the same distance from the speaker, and the center of the *FO* microphone is thus about one *inch* further than the *B&K* microphone. The one inch difference in the distance from the source results in the phase decrease estimated as follows: The phase difference ϕ in *degrees* is related to the distance difference d and the wave length λ by

$$\phi = \frac{360\, d}{\lambda}. \tag{2}$$

Differentiating this equation with respect to the frequency yields

$$\frac{d\phi}{d\nu} = \frac{360\, d}{c}, \tag{3}$$

where the relation $c = \lambda\nu$ was used, with c being the sound speed. Inserting the parametric values $d = 2.54$ *cm* and $c = 34{,}000$ *cm/sec*, one obtains $d\phi/d\nu = 0.0269$ *degrees/Hz*. This value is in a good agreement with the measured one. It enhances confidence in the tests, and in the earlier assumption that the acoustic reflection from the walls would not adversely affect the tests. It should be emphasized that the phase measurement of the frequency response does not depend on source type or on time. It will depend on the geometry of the arrangement of the source and the two microphones.

The magnitude of the frequency response function measured by using the random noise source is plotted in Fig. 7a. It is stable with a fluctuation less than 0.5 *dB* around the average value. Undesirable behavior of the average is shown at frequencies near 300 *Hz* and 480 *Hz*. This is not clearly understood presently but it is conjectured that it might be caused by electronic noise of the demodulator. Except for in the vicinity of these two frequencies, the frequency dependence of the magnitude is adequate for aeroacoustic measurements. It is fairly smooth with a decrease of 2 *dB* as the frequency reaches 2 *kHz*. This decrease is caused by the demodulator gain factor which shows a similar decrease, as displayed in Fig. 5a.

The magnitude of the frequency response function measured by using a swept sine mode is plotted in Fig. 8a. It exhibits a 5 *dB* fluctuation, which is large compared with the one in Fig. 7a. It is unlikely that this large fluctuation is caused due to the single-tone source of a swept sine mode. We believe that this fluctuation is rather time dependent as implied earlier. With the swept sine mode, the frequency response function is measured for different frequencies at different times. It is suspected that the scaling factor of the demodulator varies with time, giving rise to the time dependent magnitude fluctuation. The time dependence is also evidenced by the frequency response function measured at a different time still using the random noise source as in Fig. 9. The magnitude exhibits a 0.5 *dB* fluctuation around an average value as in Fig. 7a., but its overall value is lower by 3 *dB* than the earlier measurement.

5. CONCLUDING REMARKS

An improved performance of a new *FO* microphone was reported. Its noise floor is sufficiently low for practical application for aeroacoustic measurements. However, the frequency response function requires further improvement. We believe that the unstable behavior of the frequency response function is caused by inconsistent performance of the demodulator with time variation of the scale factor. With a new demodulator which is being fabricated by Naval Research Laboratory for NASA, we expect that the *FO* microphone will perform with an improved frequency response function. A robust multiplexed sensor head is also being designed for in-flow tests. In this design, optic fiber is implanted on an aerodynamically smooth body to minimize flow-sensor interaction, as schematically displayed in Fig. 10.

REFERENCES

1. Cho, Y. C., "Sensor Development Programs at NASA Ames Research Center," SPIE Proc. Vol. 1100, pp. 1-6, 1989.

2. Cho, Y. C., "Fiber-Optic Interferometric Acoustic Sensors for Wind Tunnel Applications," SPIE Proc. VOL. 1795, pp. 16-27, 1992.

3. Cho, Y. C., and Soderman, P. T., "Fiber-optic interferometric sensors for measurements of pressure fluctuation: Experimental evaluation," AIAA Paper 93-0738, 31st Aerospace Sciences Meeting, Reno, NV, January 11-14, 1993.

4. Layton, M. R., "A time division multiplexed fiber optic sensors networks," Vol. 1: Technical Report prepared for Naval Research Laboratory, Washington, D. C., Contract No. N00014-87-C-2027, June, 1987.

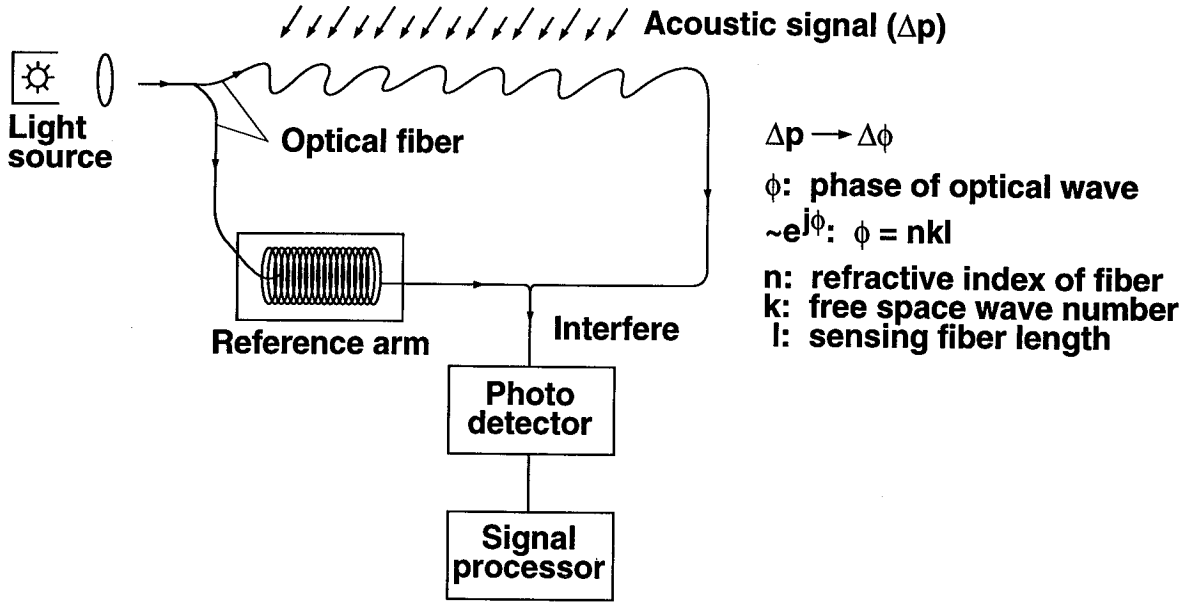

Fig. 1 Fiber optic Mach Zehnder interferometry for acoustic sensors

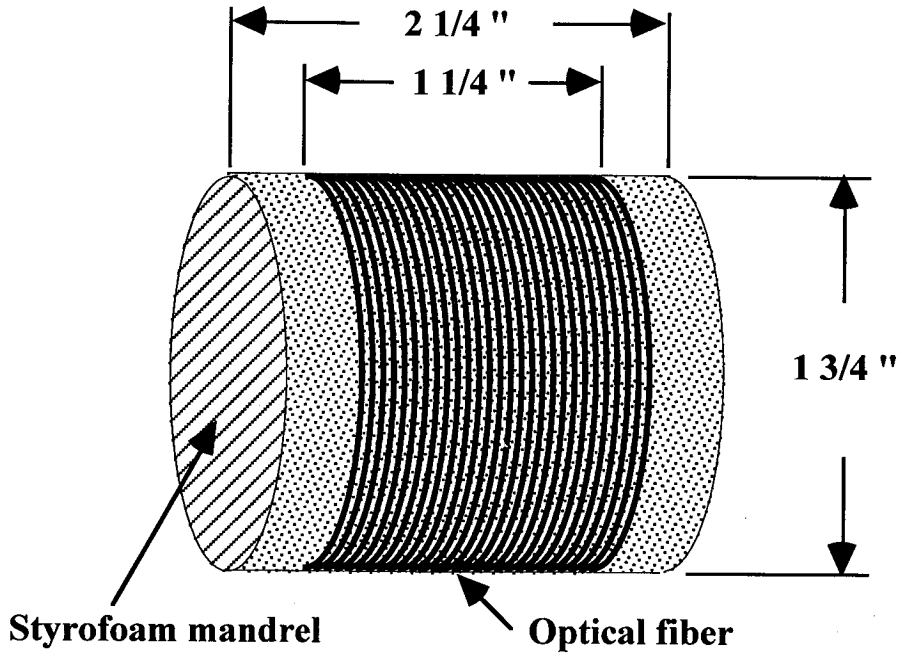

Fig. 2 Sensor head made of single mode fiber wrapped around styrofoam mandrel

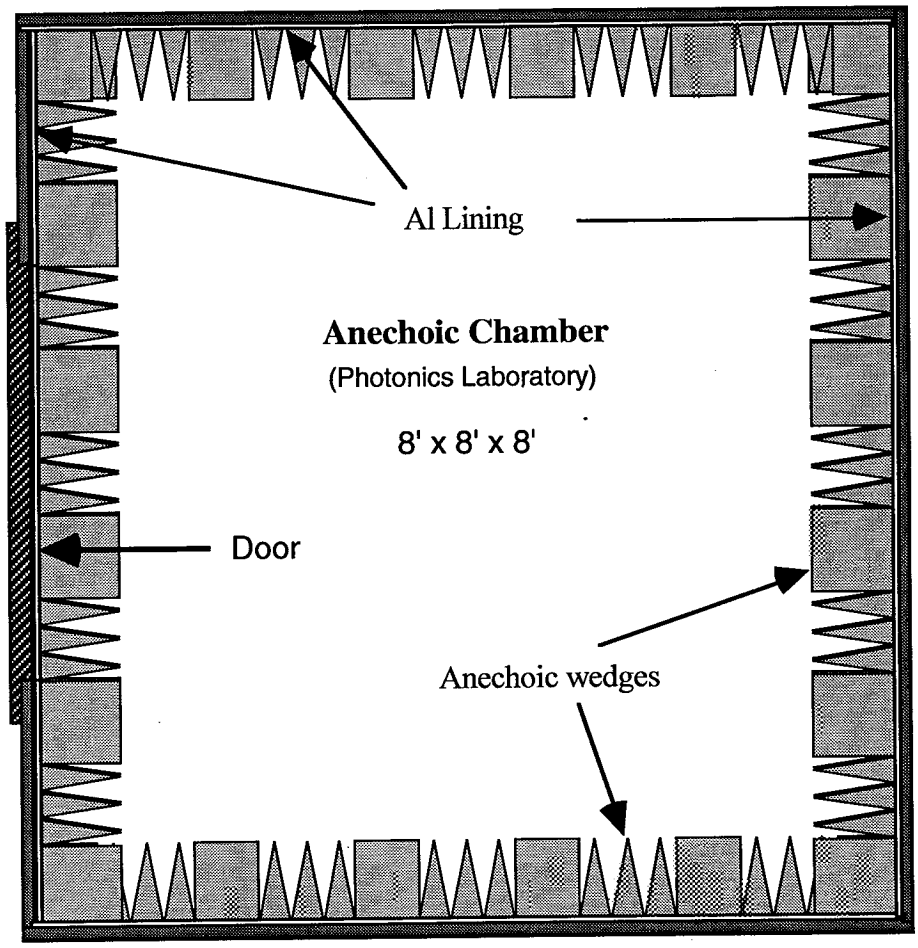

Fig. 3 Plan view of Photonics Laboratory Anechoic Chamber
NASA Ames Research Center

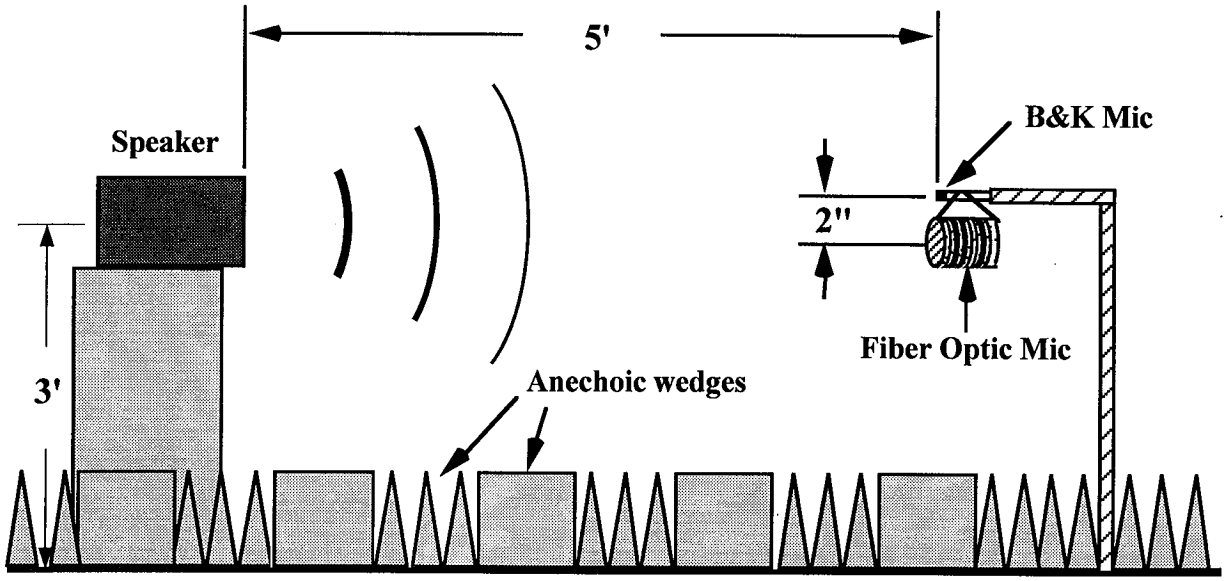

Fig. 4 Arrangement of speaker and microphones for anechoic chamber tests

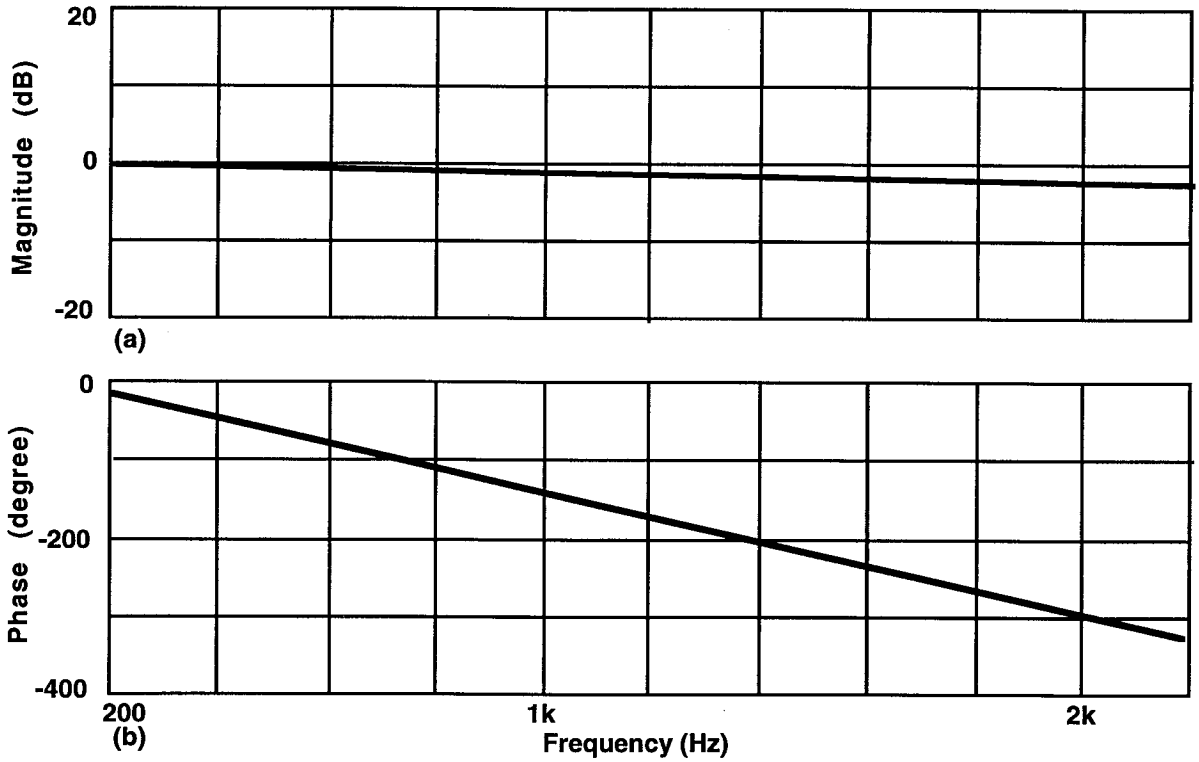

Fig. 5 Frequency response function of demodulator. a) Magnitude, b) phase.

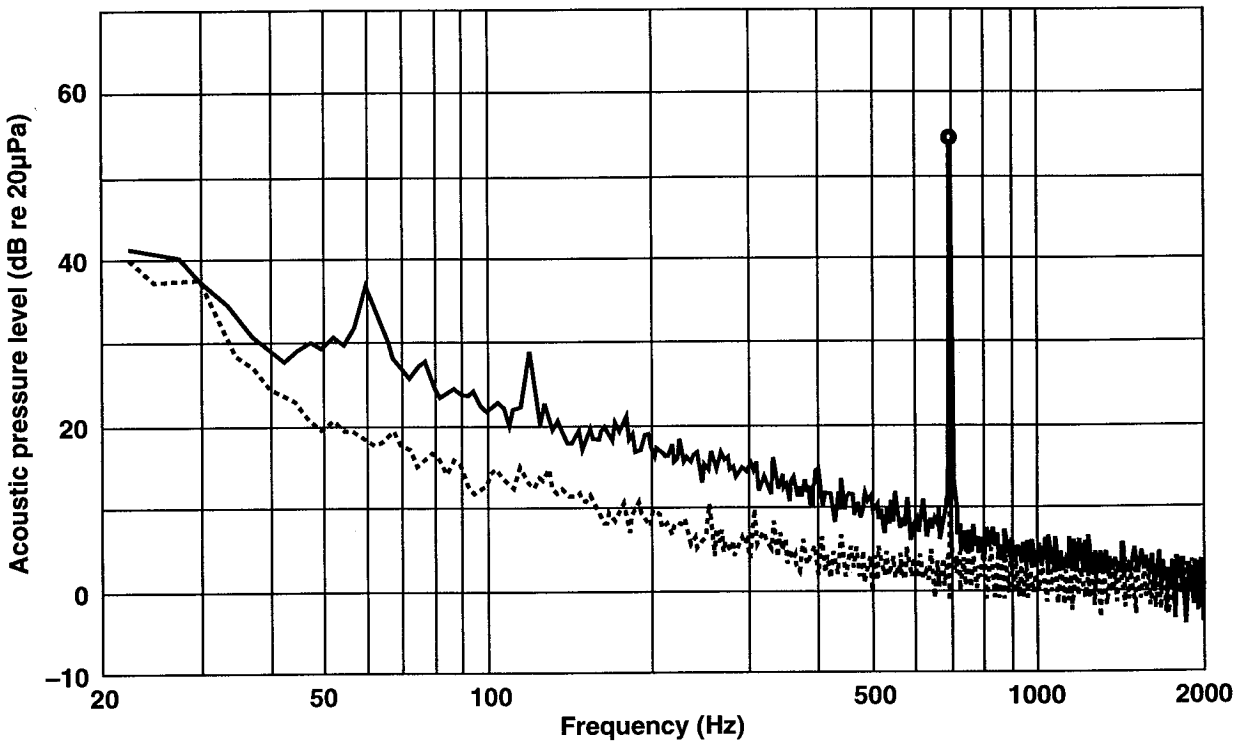

Fig. 6 Noise floor of microphones. Solid curve for fiber optic; dotted curve for B&K

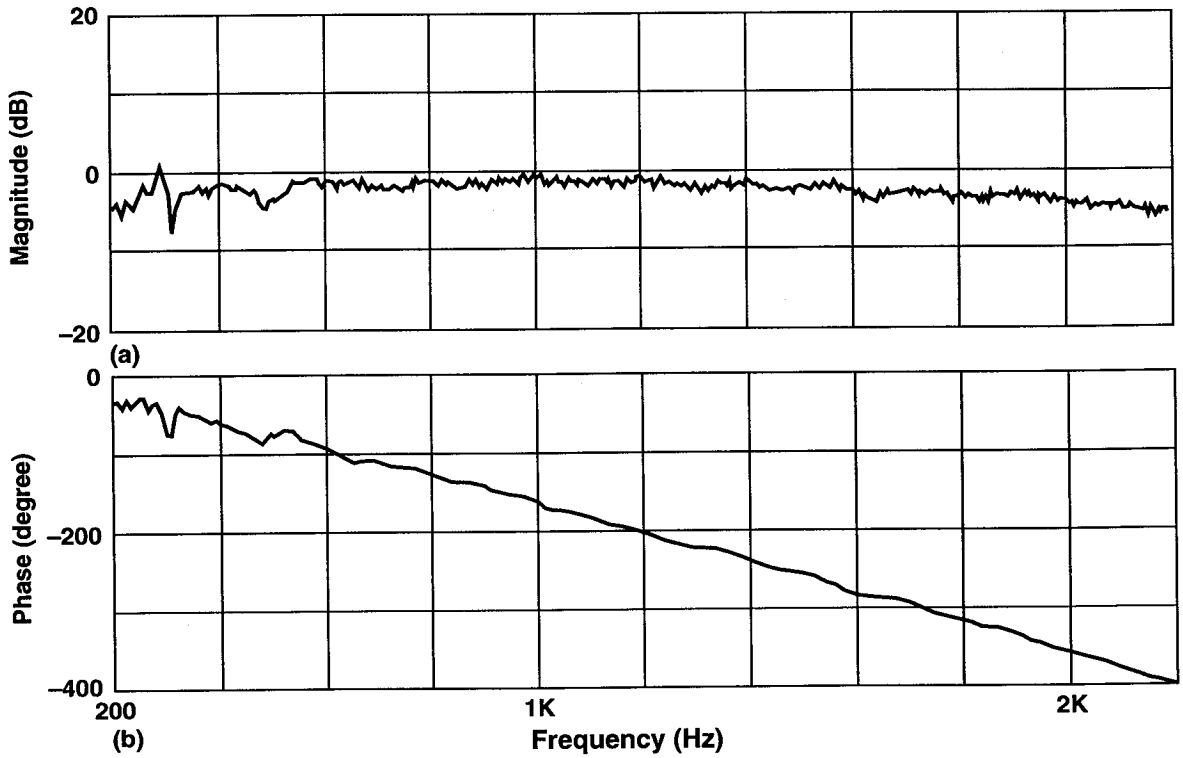

Fig. 7 Frequency response function of fiber optic microphone. a) Magnitude, b) phase. Random noise source used.

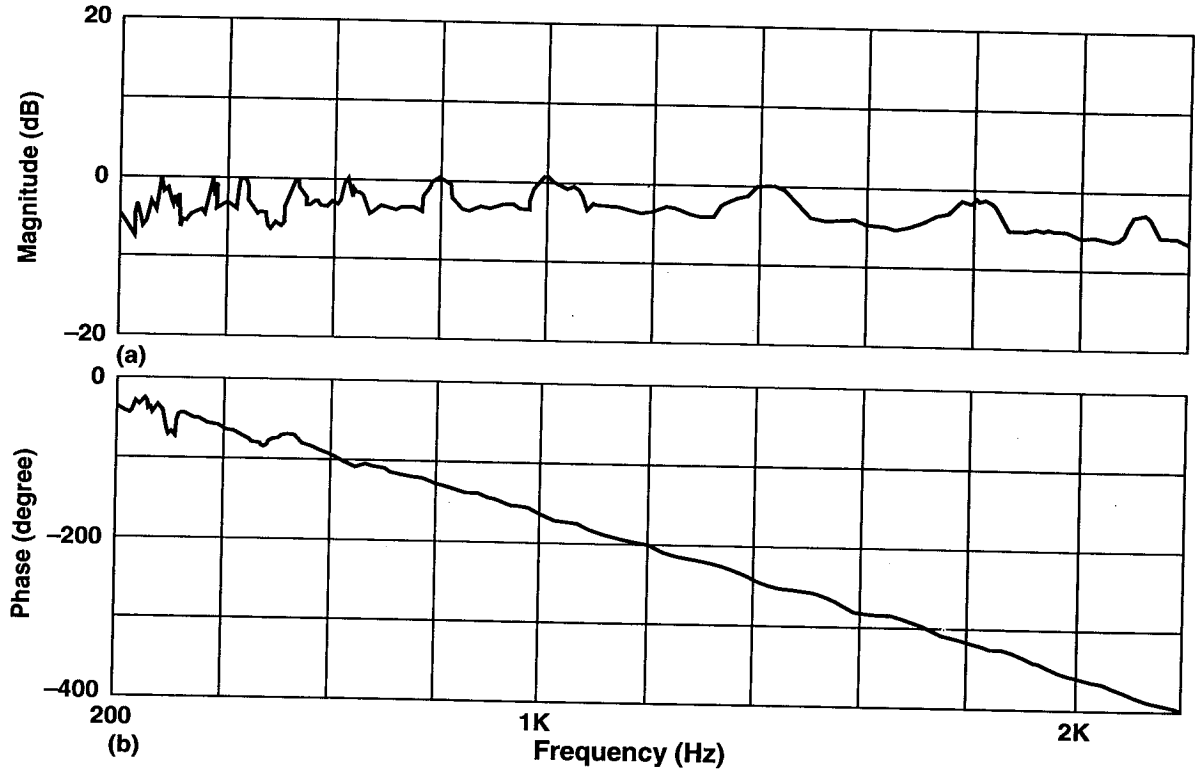

Fig. 8 Frequency response function of fiber optic microphone. a) Magnitude, b) phase. Single-tone source of swept sine mode used

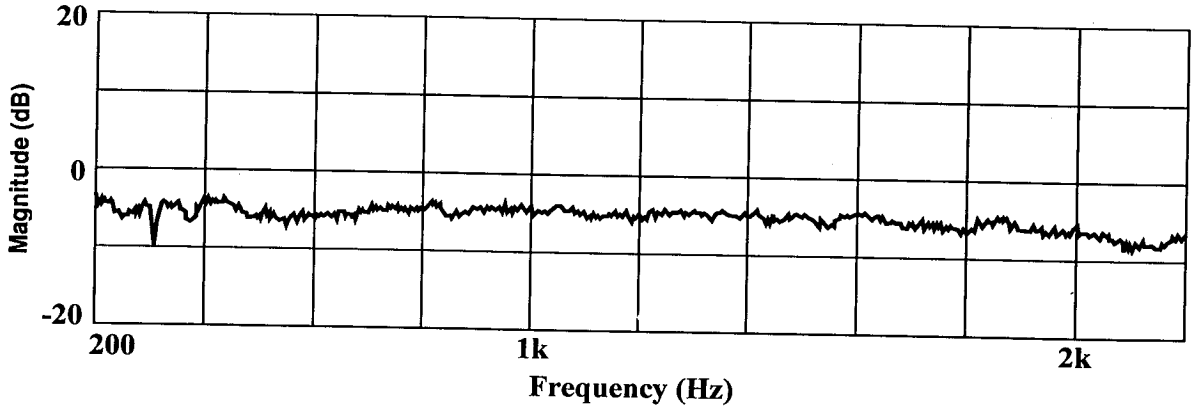

Fig. 9 Magnitude of frequency response function of fiber optic microphone, measured at a different time than one in Fig. 7. Random noise source used.

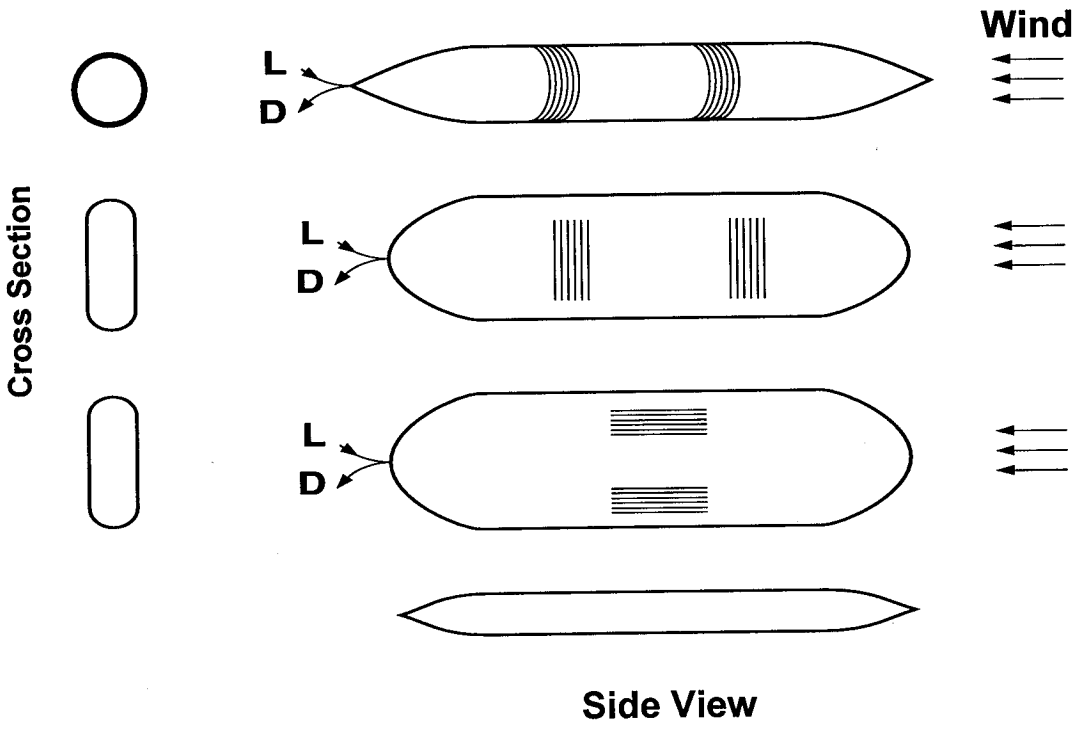

Fig. 10 Fiber optic sensor heads made of single mode fiber implanted on surface of smooth body